Inorg. Chem. **2006**, *45*, 4391–4395

Inorganic Chemistry Article

Single-Crystal Structure of the 2H-Related Perovskites $(A_{3-x}Na_x)NaBO_6$ (A = La, Pr, Nd; B = Rh, Pt)

René B. Macquart, William R. Gemmill, Matthew J. Davis, Mark D. Smith, and Hans-Conrad zur Loye*

Department of Chemistry and Biochemistry, University of South Carolina, Columbia, South Carolina 29208

Received January 18, 2006

Single crystals of $La_{2.47}Na_{1.53}RhO_6$, $Pr_{2.45}Na_{1.55}RhO_6$, $Nd_{2.45}Na_{1.55}RhO_6$, $La_2Na_2PtO_6$, and $Nd_2Na_2PtO_6$ were grown from carbonate and "wet" hydroxide fluxes. All were found to crystallize in the trigonal space group $R\bar{3}c$ and adopt the K_4CdCl_6 structure.

Introduction

$(La_{2.47}Na_{0.53})NaRhO_6$, $(Pr_{2.45}Na_{0.55})NaRhO_6$, $(Nd_{2.45}Na_{0.55})NaRhO_6$, $(La_2Na)NaPtO_6$, and $(Nd_2Na)NaPtO_6$ belong to the class of 2H-hexagonal perovskite-related oxides with the general formula $A_{3n+3m}A'_nB_{3m+n}O_{9m+6n}$, first described by Darriet and Subramanian.[1,2] $(A_{3-x}Na_x)NaBO_6$ (A = La, Pr, Nd; B = Rh, Pt) are $m = 0$ and $n = 1$ members of the above family with substitution of Na^+ ions onto the A site. These are the only examples of such oxides with rare earths on the A site[3] and are of interest because of the insight they offer into cation substitution in these compounds.

The standard cubic perovskite has the formula ABO_3 and can be thought of as a network of corner-sharing octahedra, with the A cations occupying the cubo-octahedral cavities between the octahedra. Changes in the oxygen packing of the cubic structure lead to the hexagonal perovskite structure. In terms of layer stacking, the standard cubic perovskite is composed of $[AO_3]$ layers with ABC stacking, with the B cations filling the thus formed octahedral sites. The hexagonal system (2H perovskite) is composed of $[AO_3]$ layers stacked in an AB fashion, with the B cations once again filling the octahedral sites. This results in a structure composed of infinite chains of face-sharing $[BO_6]$ octahedra extending along the *c* axis separated by chains of A cations. The general 2H-hexagonal perovskite-related oxides deviate from the standard 2H-related perovskite in that the AB packing is now composed of a tripled $[AO_3]$ layer, $[A_3O_9]$, and a modified $[A_3O_9]$ layer, $[A_3A'O_6]$. This stacking leads to chains of alternating face-sharing $[BO_6]$ octahedra and $[A'O_6]$ trigonal prisms extending down the *c* axis separated by chains of A cations. The general formula is given by $A_{3n+3m}A'_nB_{3m+n}O_{9m+6n}$, where *n* is the number of $[A_3A'O_6]$ layers and *m* is the number of $[A_3O_9]$ layers. $(La_{2.47}Na_{0.53})NaRhO_6$, $(Pr_{2.45}Na_{0.55})NaRhO_6$, $(Nd_{2.45}Na_{0.55})NaRhO_6$, $(La_2Na)NaPtO_6$, and $(Nd_2Na)NaPtO_6$ have structures that consist solely of AB-stacked $[A_3A'O_6]$ layers and, within these layers, the Na^+ cation occupies all of the A′ site and partially substitutes for the rare-earth cations on the A site. Thus, Na is also present in the chains of cations that separate the face-sharing octahedra/trigonal-prism chains.

The use of molten fluxes in the formation of single crystals has been investigated extensively.[4] Our group has had considerable success incorporating alkali and alkaline-earth metals, first- and second-row transition-metal elements, and lanthanides into a range of metal oxide structures.[5−17] This synthetic versatility is due, in large part, to the use of

* To whom correspondence should be addressed. E-mail: zurloye@mail.chem.sc.edu. Phone: +1-803-777-6916. Fax: +1-803-777-8508. Web site: http://www.chem.sc.edu.

(1) Darriet, J.; Subramanian, M. A. *J. Mater. Chem.* **1995**, *5*, 543.
(2) Perez-Mato, J. M.; Zakhour-Nakhl, M.; Weill, F.; Darriet, J. *J. Mater. Chem.* **1999**, *9*, 2795.
(3) Stitzer, K. E.; Darriet, J.; zur Loye, H.-C. *Curr. Opin. Solid State Mater. Sci.* **2001**, *5*, 535.
(4) Elwell, D.; Scheel, H. J. *Crystal Growth from High-Temperature Solutions*; Academic Press: New York, 1975.
(5) Claridge, J. B.; Layland, R. C.; Henley, W. H.; zur Loye, H.-C. *Chem. Mater.* **1999**, *11*, 1376.
(6) zur Loye, H.-C.; Layland, R. C.; Smith, M. D.; Claridge, J. B. *J. Cryst. Growth* **2000**, *211*, 452.
(7) Stitzer, K. E.; El Abed, A.; Darriet, J.; zur Loye, H.-C. *J. Am. Chem. Soc.* **2001**, *123*, 8790.
(8) Davis, M. J.; Smith, M. D.; zur Loye, H.-C. *Inorg. Chem.* **2003**, *42*, 6980.
(9) Stitzer, K. E.; Gemmill, W. R.; Smith, M. D.; zur Loye, H.-C. *J. Solid State Chem.* **2003**, *175*, 39.
(10) Kim, S.-J.; Smith, M. D.; Darriet, J.; zur Loye, H.-C. *J. Solid State Chem.* **2004**, *177*, 1493.
(11) Gemmill, W. R.; Smith, M. D.; zur Loye, H.-C. *Inorg. Chem.* **2004**, *43*, 4254.
(12) Mwamuka, J. N.; Gemmill, W. R.; Stitzer, K. E.; Smith, M. D.; zur Loye, H.-C. *J. Alloys Compd.* **2004**, *377*, 91.
(13) Gemmill, W. R.; Smith, M. D.; zur Loye, H.-C. *J. Solid State Chem.* **2004**, *177*, 3560.

10.1021/ic060105o CCC: $33.50
Published on Web 05/02/2006

carbonate and hydroxide fluxes. Of particular interest to us is the ability of carbonates and "wet" hydroxide fluxes to dissolve platinum group metals and lanthanides.[5,12−20] We have recently reported on the use of a K_2CO_3 flux in the growth of $RERhO_3$ (RE = La, Pr, Nd, Sm, Eu, Tb) single crystals.[21] Whereas the K^+ ions are too large to interact with the orthorhodite structure, it has been shown that Na^+ ions can substitute into 2H-related perovskite oxides, for example, $(NaLa_2)NaPtO_6$[8] and Ca_3NaRuO_6.[22] In light of these results, the use of Na_2CO_3 and "wet" NaOH fluxes was investigated for their ability to dissolve and react with a range of rare-earth oxides and platinum group metals. Both flux media have a relatively low toxicity and are easy to remove postreaction by washing with water. The carbonate flux requires heating to around 1050 °C, while the hydroxide flux dissolves the reactants readily at much lower temperatures, typically 600−700 °C. However, the success of the hydroxide flux in dissolving the reactants, particularly rare-earth oxides is due to the acid−base properties of the flux. Specifically, an acidic hydroxide flux[19] is required to dissolve rare-earth oxides, which, according to the Lux−Flood concept of oxoacidity,[23,24] means a "wet" flux. Consequently, in addition to the reactants and the NaOH flux, a small quantity of water is necessary to ensure the desired crystal growth.

There are a large number of $m = 0$ and $n = 1$ $A_{3n+3m}A'_{n}B_{3m+n}O_{9m+6n}$ ($A_3A'BO_6$) oxides.[3] While the A′ and B site cations have a wide range of flexibility with combinations ranging from A'^{+}/B^{5+} (Ca_3LiRuO_6[25,26] and Ba_3NaBiO_6[27]) and A'^{2+}/B^{4+} (Sr_3MgIrO_6[28]) to A'^{3+}/B^{3+} (Sr_3YRhO_6[29]) and A'^{4+}/B^{2+} (Sr_3PbNiO_6[6,30]), the A site cations have always been the alkaline-earth metals Ca, Sr, and Ba.[3] To the best of our knowledge, the title compounds are unique in two respects. First, they contain a rare earth on the A site and, second, the A site is occupied by two separate elements. The growth and structural characterization of $(La_2Na)NaPtO_6$ has been communicated by our group previously.[8] Here, we report for the first time the related Rh and Pt analogues $La_{2.47}Na_{1.53}RhO_6$, $Pr_{2.45}Na_{1.55}RhO_6$, $Nd_{2.45}Na_{1.55}RhO_6$, and $Nd_2Na_2PtO_6$ grown using two distinct flux media and describe some general structural trends observed within the group.

Experimental Procedures

Two different flux preparation methods were used in the growth of the $(A_{3-x}Na_x)NaBO_6$ (A = La, Pr, Nd; B = Rh, Pt) crystals. The first involved the growth of single crystals from a "wet" hydroxide flux, resulting in $La_{2.47}Na_{1.53}RhO_6$, $La_2Na_2PtO_6$, and $Nd_2Na_2PtO_6$. The second method, using a Na_2CO_3 flux, produced $Pr_{2.45}Na_{1.55}RhO_6$ and $Nd_{2.45}Na_{1.55}RhO_6$ crystals as well as poorer quality $(La_{3-x}Na_x)NaRhO_6$ crystals. In both cases, RE_2O_3 (RE = La, Nd; Alfa Aesar, 99.9%) was initially heated to 1000 °C for 15 h to ensure dryness. Pr_2O_3 was obtained from Pr_6O_{11} (Alfa Aesar, 99.9%) by heating it in a tube furnace under flowing H_2 (5%)/N_2 (95%) at 1000 °C for 15 h, cooling it, grinding it up, and then heating it again at 1000 °C for another 15 h under flowing H_2 (5%)/N_2 (95%). RE_2O_3 (RE = La, Pr, Nd) was stored in a vacuum desiccator when not in use. Rh metal (Engelhard, powdered 99.987%) was used to grow $Pr_{2.45}Na_{1.55}RhO_6$ and $Nd_{2.45}Na_{1.55}RhO_6$, while Rh_2O_3 (prepared by heating powdered Rh metal at 1000 °C for 24 h in air) was used for $La_{2.47}Na_{1.53}RhO_6$. Both of the Pt analogues were grown using $(NH_4)_2PtCl_6$ (prepared according to Kaufman[31]).

Method 1. RE_2O_3 (0.5 mmol) and $(NH_4)_2PtCl_6$ (1 mmol) or Rh_2O_3 (0.5 mmol) were added to a silver crucible. NaOH (10 g; Fisher ACS reagent) was added on top of these reagents followed by deionized water (2 g). The crucible was covered with a silver lid, heated in air at a rate of 5 °C min^{-1} (Pt analogues) or 10 °C min^{-1} (Rh analogue) to 700 °C, and held there for 12 h before turning off the furnace and allowing it to cool to room temperature. Small yellow crystals of $La_2Na_2PtO_6$ (60 × 40 μm) and $Nd_2Na_2PtO_6$ (30 × 20 μm) and small brown-green crystals of $La_{2.47}Na_{1.53}RhO_6$ (50 × 40 μm) were isolated from the flux matrix by washing with deionized water with the aid of sonication.

Method 2. Rh metal (1 mmol) and RE_2O_3 (RE = La, Pr, Nd; 1.25 mmol) were ground in an acetone slurry with an agate mortar and pestle. The reactants were placed in an alumina crucible and covered with anhydrous Na_2CO_3 (105 mmol; Fisher Scientific, 99.8%). The crucible was covered with an alumina lid, heated in a tube furnace from room temperature to 1050 °C at a rate of 600 °C h^{-1}, held at 1050 °C for 24 h, then cooled to 800 °C at a rate of 15 °C h^{-1}, held at 800 °C for 1 h, and then step cooled to room temperature by cutting power to the furnace elements. The crucible was immersed in deionized water and sonicated in order to dissolve the flux. The resulting material was filtered under suction and washed with more deionized water followed by a final washing with a small amount of acetone. Small black $Pr_{2.45}Na_{1.55}RhO_6$ (50 × 40 μm) and $Nd_{2.45}Na_{1.55}RhO_6$ (40 × 30 μm) crystals were isolated.

The morphology and composition of the crystals were examined using scanning electron microscopy (SEM) and energy-dispersive X-ray analysis (EDS). Measurements were performed with a Quanta ESEM 200. Once an approximate composition was confirmed with EDS, the crystals were then examined using single-crystal X-ray

(14) Gemmill, W. R.; Smith, M. D.; Prozorov, R.; zur Loye, H.-C. *Inorg. Chem.* **2005**, *44*, 2639.
(15) Mugavero, S. J., III; Puzdrjakova, I. V.; Smith, M. D.; zur Loye, H.-C. *Acta Crystallogr.* **2005**, *E61*, i3.
(16) Mugavero, S. J., III; Smith, M. D.; zur Loye, H.-C. *J. Solid State Chem.* **2005**, *178*, 200.
(17) Mugavero, S. J., III; Smith, M. D.; zur Loye, H.-C. *J. Solid State Chem.* **2005**, *178*, 3176.
(18) Stitzer, K. S.; Smith, M. D.; zur Loye, H.-C. *J. Alloys Compd.* **2002**, *338*, 104.
(19) Keller, S. W.; Carlson, V. A.; Sandford, D.; Stenzel, F.; Stacy, A. M.; Kwei, G. H.; Alario-Franco, M. *J. Am. Chem. Soc.* **1994**, *116*, 8070.
(20) Luce, J. L.; Stacy, A. M. *Chem. Mater.* **1997**, *9*, 1508.
(21) Macquart, R. B.; Smith, M. D.; zur Loye, H.-C. *Cryst. Growth Des.* **2006**, in press.
(22) Claridge, J. B.; Layland, R. C.; Adams, R. D.; zur Loye, H.-C. *Z. Anorg. Allg. Chem.* **1997**, *623*, 1131.
(23) Lux, H. *Z. Elektrochem.* **1939**, *45*, 303.
(24) Flood, H.; Forland, T. *Acta Chem. Scand.* **1947**, *1*, 592.
(25) Darriet, J.; Grasset, F.; Battle, P. D. *Mater. Res. Bull.* **1997**, *32*, 139.
(26) Battle, P. D.; Blake, G. R.; Burley, J. C.; Cussen, E. J.; Sloan, J.; Vente, J. F.; Darriet, J.; Weill, F. Commensurate and Incommensurate Oxide Structures Related to 2H Perovskite. *Mater. Res. Soc. Symp. Proc.* **1999**, *547*, 45.
(27) Carlson, V. A.; Stacy, A. M. *J. Solid State Chem.* **1992**, *96*, 332.
(28) Núñez, P.; Trail, S.; zur Loye, H.-C. *J. Solid State Chem.* **1997**, *130*, 35.
(29) Layland, R. C.; Kirkland, S. L.; Núñez, P.; zur Loye, H.-C. *J. Solid State Chem.* **1998**, *139*, 416.
(30) Smith, M. D.; Stalick, J. K.; zur Loye, H.-C. *Chem. Mater.* **1999**, *11*, 2984.
(31) Kaufman, G. S. *Inorganic Syntheses*; McGraw-Hill: New York, 1967; Vol. 9, p 182.

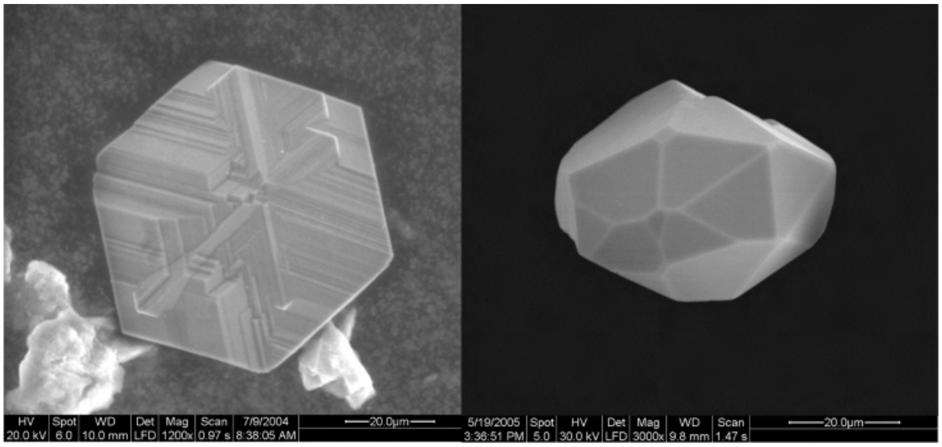

Figure 1. SEM image of a single crystal of ($La_{2.47}Na_{0.53}$)$NaRhO_6$ amidst a small quantity of matrix material (left) and a single crystal of ($Nd_{2.45}Na_{0.55}$)-$NaRhO_6$ (right).

Table 1. Collection Parameters, Structural Data, and Refinement Statistics for ($A_{3-x}Na_x$)$NaBO_6$ (A = La, Pr, Nd; B = Rh, Pt)

empirical formula	$La_{2.47}Na_{1.53}RhO_6$	$Pr_{2.45}Na_{1.55}RhO_6$	$Nd_{2.45}Na_{1.55}RhO_6$	$La_2Na_2PtO_6$	$Nd_2Na_2PtO_6$
fw (g mol^{-1})	576.81	579.58	588.60	614.89	625.55
T (K)	294(1)	150(1)	294(2)	293(2)	294(2)
space group	$R\bar{3}c$	$R\bar{3}c$	$R\bar{3}c$	$R\bar{3}c$	$R\bar{3}c$
unit cell dimens					
a (Å)	9.4770(2)	9.3534(2)	9.3352(9)	9.5031(2)	9.3618(3)
b (Å)	9.4770(2)	9.3534(2)	9.3352(9)	9.5031(2)	9.3618(3)
c (Å)	11.4901(4)	11.3386(5)	11.304(2)	11.4625(5)	11.2959(6)
V (Å^3)	893.71(4)	859.07(5)	853.1(2)	896.48(5)	857.37(6)
Z	6	6	6	6	6
D(calcd) (g cm^{-3})	6.430	6.722	6.874	6.834	7.269
abs coeff (mm^{-1})	20.152	23.397	25.002	37.498	42.427
F(000)	1503	1527	1544	1572	1608
cryst size (mm)	0.05 × 0.04 × 0.02	0.05 × 0.04 × 0.02	0.04 × 0.03 × 0.02	0.06 × 0.04 × 0.02	0.03 × 0.02 × 0.02
θ range for data collcn (deg)	4.30−35.21	4.36−35.18	4.37−37.76	4.29−33.21	4.35−28.30
reflns collected	5640	5657	5811	2708	2742
independent reflns	452 (R_{int} = 0.0424)	432 (R_{int} = 0.0445)	513 (R_{int} = 0.0398)	390 (R_{int} = 0.0339)	246 (R_{int} = 0.0496)
GOF on F^2	1.162	1.263	1.057	1.048	1.142
final R indices [$I > 2\sigma(I)$]	R_1 = 0.0293, wR_2 = 0.0533	R_1 = 0.0279, wR_2 = 0.0446	R_1 = 0.0257, wR_2 = 0.0449	R_1 = 0.0234, wR_2 = 0.0457	R_1 = 0.0262, wR_2 = 0.0607
R indices (all data)	R_1 = 0.0360, wR_2 = 0.0551	R_1 = 0.0322, wR_2 = 0.0453	R_1 = 0.0300, wR_2 = 0.0460	R_1 = 0.0307, wR_2 = 0.0648	R_1 = 0.0275, wR_2 = 0.0615
largest diffraction peak and hole (e Å^{-3})	2.168 and −1.693	1.486 and −1.889	1.869 and −1.682	2.17 and −2.39	4.201 and −2.502

diffraction techniques. Descriptions of the single-crystal refinement process for each compound can be found in the Supporting Information. The interested reader should refer, in particular, to the description of the solution of the single-crystal structure of $La_2Na_2PtO_6$ given in the Supporting Information. Note that this material has been published previously[8] but is included here because it is representative of the process employed in the solution of the subsequently solved crystal structures. A brief description of the collection of data for $Nd_{2.45}Na_{1.55}RhO_6$ is given here as a representative guide for the four new crystals.

X-ray intensity data from a black block of approximate dimensions 0.04 × 0.03 × 0.02 mm^3 were measured at 294(2) K on a Bruker SMART APEX CCD-based diffractometer (Mo Kα radiation, λ = 0.710 73 Å).[32] The data collection covered 100% of reciprocal space to $2\theta_{max}$ = 75.52° (R_{int} = 0.0398; average redundancy = 10.8). Raw data frame integration and Lorentz and polarization corrections were performed with *SAINT+*.[32] Final unit cell parameters were determined by least-squares refinement of 2687 reflections with $I > 5\sigma(I)$ from the data set. Analysis of the data showed negligible crystal decay during collection. The data were corrected for absorption effects with *SADABS*.[32] Refinement by full-matrix least squares against F^2 was carried out with *SHELXTL*.[33] A summary of the collection parameters for ($A_{3-x}Na_x$)$NaBO_6$ (A = La, Pr, Nd; B = Rh, Pt) is given in Table 1.

The magnetic susceptibility of (Nd_2Na)$NaPtO_6$ was measured using a Quantum Design MPMS XL SQUID magnetometer. For the magnetic measurements, loose crystals of (Nd_2Na)$NaPtO_6$ were placed into a gelatin capsule, which was placed inside a plastic straw. The sample was measured under both zero-field-cooled and field-cooled conditions in an applied field of 10 kG. The very small diamagnetic contribution of the gelatin capsule containing the sample had a negligible contribution to the overall magnetization, which was dominated by the sample signal.

Results and Discussion

($A_{3-x}Na_x$)$NaBO_6$ (A = La, Pr, Nd; B = Rh, Pt) were all found to crystallize in the trigonal space group $R\bar{3}c$ with the K_4CdCl_6 structure.[34] Figure 1 shows SEM images of two

(32) *SMART*, version 5.625; *SADABS*, version 2.05; Bruker Analytical X-ray Systems, Inc.: Madison, WI, 2001.

(33) Sheldrick, G. M. *SHELXTL*, version 6.1; Bruker Analytical X-ray Systems, Inc.: Madison, WI, 2000.

(34) Bergerhoff, G.; Schmitz-DuMont, O. *Naturwissenschaften* **1954**, *41*, 280.

Table 2. Refined Atomic Composition, Coordinates,[a] and Equivalent Isotropic Atomic Displacement Parameters for $(A_{3-x}Na_x)NaBO_6$ (A = La, Pr, Nd; B = Rh, Pt)

	x	y	z	U_{eq}[b]	occupancy
			$(La_{2.47(2)}Na_{0.53(2)})NaRhO_6$		
La(1)	0.3640(1)	0	$^1/_4$	0.010(1)	0.822(5)
Na(1)	0.3640(1)	0	$^1/_4$	0.010(1)	0.178(5)
Na(2)	0	0	$^1/_4$	0.013(1)	1
Rh(1)	0	0	0	0.006(1)	1
O(1)	0.1900(4)	0.0272(4)	0.1045(3)	0.012(1)	1
			$(Pr_{2.45(2)}Na_{0.55(2)})NaRhO_6$		
Pr(1)	0.3635(1)	0	$^1/_4$	0.007(1)	0.816(5)
Na(1)	0.3635(1)	0	$^1/_4$	0.007(1)	0.184(5)
Na(2)	0	0	$^1/_4$	0.009(1)	1
Rh(1)	0	0	0	0.004(1)	1
O(1)	0.1934(4)	0.0299(4)	0.1044(3)	0.009(1)	1
			$(Nd_{2.45(1)}Na_{0.55(1)})NaRhO_6$		
Nd(1)	0.3638(1)	0	$^1/_4$	0.009(1)	0.818(4)
Na(1)	0.3638(1)	0	$^1/_4$	0.009(1)	0.182(4)
Na(2)	0	0	$^1/_4$	0.012(1)	1
Rh(1)	0	0	0	0.006(1)	1
O(1)	0.1941(3)	0.0298(4)	0.1044(2)	0.011(1)	1
			$(La_2Na)NaPtO_6$		
La(1)	0.3612(4)	0	$^1/_4$	0.0097(2)	2/3
Na(1)	0.3612(4)	0	$^1/_4$	0.0097(2)	1/3
Na(2)	0	0	$^1/_4$	0.0113(9)	1
Pt(1)	0	0	0	0.0050(1)	1
O(1)	0.1863(5)	0.0255(5)	0.1025(3)	0.0126(7)	1
			$(Nd_2Na)NaPtO_6$		
Nd(1)	0.3607(1)	0	$^1/_4$	0.010(1)	2/3
Na(1)	0.3607(1)	0	$^1/_4$	0.010(1)	1/3
Na(2)	0	0	$^1/_4$	0.011(2)	1
Pt(1)	0	0	0	0.006(1)	1
O(1)	0.1905(8)	0.0284(8)	0.1025(6)	0.013(1)	1

[a] A and Na(1) at the 18*e* site, Na(2) at the 6*a* site, B(1) at the 6*b* site, and O(1) at the 36*f* site of $R\bar{3}c$. [b] U_{eq} is defined as one-third of the trace of the orthogonalized $\mathbf{U}_{ij}$ tensor.

crystals displaying geometry typical of hexagonal symmetry, $(La_{2.47}Na_{0.53})NaRhO_6$ and $(Nd_{2.45}Na_{0.55})NaRhO_6$. The lattice parameters and quality of fit for each compound are given in Table 1.

Table 2 lists the refined compositions, atomic coordinates, and equivalent isotropic atomic displacement parameters for $(A_{3-x}Na_x)NaBO_6$ (A = La, Pr, Nd; B = Rh, Pt) calculated from the single-crystal X-ray diffraction data. In each case, the occupancies of the rare earth and the Na(1) atom on the mixed 18*e* site were allowed to refine but were constrained to sum to unity. From these results, the stoichiometries of the A site cations for each of the compounds were obtained. More detail on this can be found in the Supporting Information. Figure 2 shows the structure of $(Nd_{2.45}Na_{0.55})NaRhO_6$, representative of all of the crystal compositions. Regular $[RhO_6]$ octahedra share faces with distorted $[NaO_6]$ trigonal prisms to form polyhedral chains along the *c* axis. These polyhedral chains are surrounded by Nd/Na(1) cations coordinated to eight O anions such that they form a polyhedral spiral along the *c* axis composed of $[(Nd/Na(1))\text{-}O_8]$ units. Table 3 lists the refined stoichiometries, A/Na(1)−O atomic distances for the eight-coordinate A/Na(1) cation site, the distance between the A site cation and its nearest non-O neighbor, the B−O bond lengths for the $[BO_6]$ regular octahedra, and the Na(2)−O bond lengths for the Na(2)-centered distorted trigonal prisms. The B−O and Na(2)−O bond lengths fall within the standard range for these atom types. For a six-coordinate cation, the average Rh−O bond length is 1.88−2.049 Å, for Pt−O 1.98−2.029 Å, and for Na−O 2.37−2.466 Å.[35,36] Figures 3 and 4 show comparisons of these values as a function of the rare-earth cation size. As the size of the rare-earth cation on the A site increases, there is a general increase in the A/Na(1)−O, B−O, and Na(2)−O bond lengths, which coincides with an increase in the unit cell volume (Figure 5). The slightly larger Pt (ionic radius 0.57 Å) cations on the B site increase the overall volume compared to the Rh cations (ionic radius 0.55 Å).

On the basis of the concept of charge neutrality, the overall contribution of the cation charges in $(A_{3-x}Na_x)NaBO_6$ (A = La, Pr, Nd; B = Rh, Pt) must sum to +12 to offset the six O^{2-} anions. In the case of the Pt-containing analogues and assuming that Na has a 1+ charge and the rare earth a 3+

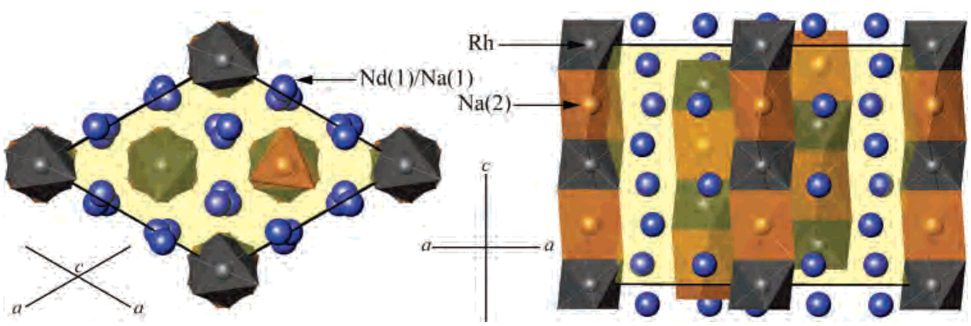

Figure 2. Structure of $(Nd_{2.45}Na_{0.55})NaRhO_6$ characteristic of $(A_{3-x}Na_x)NaBO_6$ (A = La, Pr, Nd; B = Rh, Pt) looking down the *c* axis (left) and the [110] axis (right). Atoms are marked. Note that there is mixing on the 18e site occupied by Nd(1) and Na(1) atoms.

Table 3. Selected Atomic Distances and Bond Lengths (Å) for $(A_{3-x}Na_x)NaBO_6$ (A = La, Pr, Nd; B = Rh, Pt)

	$(La_{2.47}Na_{0.53})NaRhO_6$	$(Pr_{2.45}Na_{0.55})NaRhO_6$	$(Nd_{2.45}Na_{0.55})NaRhO_6$	$La_2Na_2PtO_6$	$(Nd_2Na)NaPtO_6$
A/Na(1)−O(1) × 2	2.450(3)	2.404(3)	2.395(3)	2.467(5)	2.410(7)
A/Na(1)−O(1) × 2	2.542(3)	2.498(3)	2.487(3)	2.541(4)	2.491(7)
A/Na(1)−O(1) × 2	2.553(4)	2.501(3)	2.498(3)	2.564(4)	2.505(6)
A/Na(1)−O(1) × 2	2.719(4)	2.709(3)	2.701(3)	2.733(5)	2.720(7)
A/Na(1)−Rh	3.1723(2)	3.1327(2)	3.1253(3)	3.190(2)	3.1451(4)
B(1)−O(1) × 6	2.071(3)	2.060(3)	2.061(3)	2.036(4)	2.029(6)
Na(2)−O(1) × 6	2.375(3)	2.360(3)	2.359(3)	2.371(4)	2.357(7)

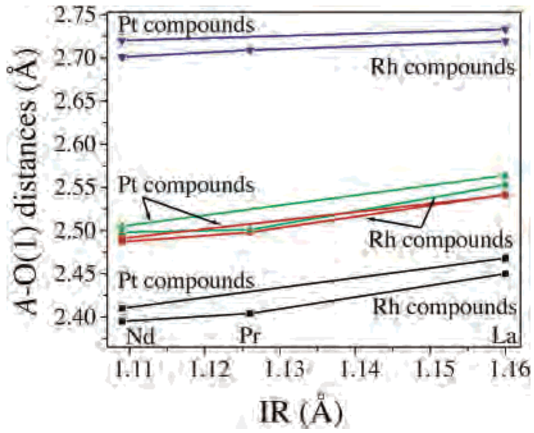

Figure 3. A−O(1) bond distances for $(A_{3-x}Na_x)NaBO_6$ (A = La, Pr, Nd; B = Rh, Pt).

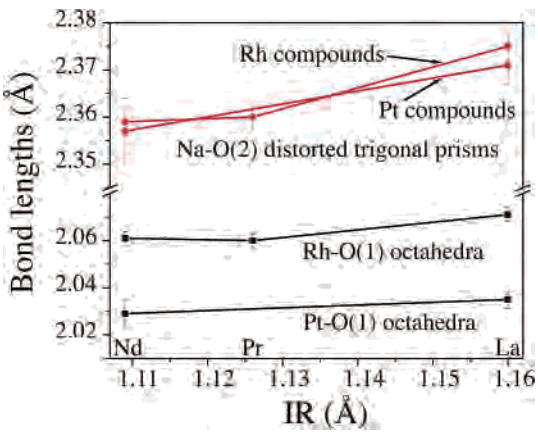

Figure 4. Polyhedral bond lengths in $(A_{3-x}Na_x)NaBO_6$ (A = La, Pr, Nd; B = Rh, Pt) as a function of the rare-earth cation size.

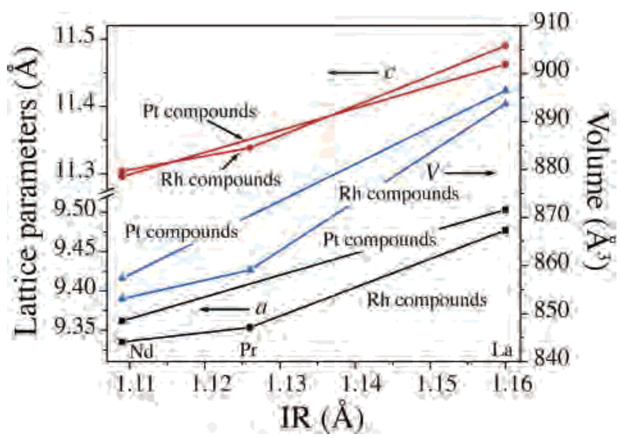

Figure 5. Lattice parameters and volume of $(A_{3-x}Na_x)NaBO_6$ (A = La, Pr, Nd; B = Rh, Pt) as a function of the rare-earth cation size.

charge, this results in Pt^{4+} cations. Assuming standard charges of the rare-earth and Na cations and given the constraints used in the single-crystal refinement process, the Rh-containing crystals contain a charge discrepancy, suggesting the presence of a small amount of Rh^{4+} among the predominantly Rh^{3+} cations with overall Rh charges of +3.06, +3.10, and +3.10 for the La, Pr, and Nd analogues, respectively. Alternately, the refined site occupancies on the A site may be slightly off, accounting for the observed discrepancy. It is worth noting that it is only on account of the mixing of the 3+ rare-earth cations and the Na^+ cations on the A site that the rare-earth cations are able to occupy the site. The similarity in size between the Na^+ (ionic radius 1.18 Å), La^{3+} (1.16 Å), Pr^{3+} (1.126 Å), and Nd^{3+} (1.109 Å)[36] cations helps facilitate the mixing. Given that the only other cations found to substitute onto the A site are Ca^{2+} (ionic radius 1.12 Å), Sr^{2+} (1.26 Å), and Ba^{2+} (1.42 Å),[3] this suggests not only a charge constraint but also a size limit on which cations are suitable. Exploration of other divalent cations such as Pb^{2+} (ionic radius 1.29 Å), Cd^{2+} (1.10 Å), and mixed mono/trivalent combinations of approximately the same size may lead to new compounds.

The temperature dependence of both the susceptibility and inverse susceptibility of $(Nd_2Na)NaPtO_6$ measured in an applied field of 10 kG is shown in the Supporting Information. There is no indication of any magnetic transition down to the lowest measured temperature, 2 K. Fitting the high-temperature susceptibility (100 K < T < 300 K) to the Curie−Weiss law yields the observed magnetic moment of $\mu_{eff} = 5.06\ \mu_B$ in good agreement with the theoretical value of 5.12 μ_B. The theoretical moment is calculated by taking the square root of the sum of the squares of the moments of the contributing magnetic cations (Nd^{3+} and Nd^{3+}), $\mu_{eff} = [(\mu_B\ Nd^{3+})^2 + (\mu_B\ Nd^{3+})^2]^{1/2} = [(3.62)^2 + (3.62)^2]^{1/2} = 5.12\ \mu_B$. As expected, there is no magnetic coupling and all we observe is the moment of noninteracting rare-earth cations.

Conclusions

We have demonstrated the growth of single crystals of the 2H-hexagonal perovskite-related oxides $(La_{2.47}Na_{0.53})NaRhO_6$, $(Pr_{2.45}Na_{0.55})NaRhO_6$, $(Nd_{2.45}Na_{0.55})NaRhO_6$, $(La_2Na)NaPtO_6$, and $(Nd_2Na)NaPtO_6$ using two distinct flux media, a "wet" hydroxide flux, and a carbonate flux. These compounds are unique in that, despite the large number of examples of $A_{3n+3m}A'_nB_{3m+n}O_{9m+6n}$ ($m = 0$ and $n = 1$) oxides, these are the only ones with rare earths on the A site and additionally are the only examples with two distinct cations on that site.

Acknowledgment. Financial support from the Department of Energy through Grant DE-FG02-04ER46122 and from the National Science Foundation through Grant DMR:0450103 is gratefully acknowledged.

Supporting Information Available: A description of the single-crystal refinement strategy for each of the five crystals, a plot of magnetic susceptibility versus temperature for $(Nd_2Na)NaPtO_6$ measured in an applied field of 10 kG, and X-ray crystallographic files in CIF format. This material is available free of charge via the Internet at http://pubs.acs.org. Four X-ray crystallographic information files (CIF) for $(La_{2.47}Na_{0.53})NaRhO_6$, $(Pr_{2.45}Na_{0.55})NaRhO_6$, $(Nd_{2.45}Na_{0.55})NaRhO_6$, and $(Nd_2Na)NaPtO_6$ with reference nos. 416108, 416109, 416110, and 416111 have been deposited at the ICSD. The CIF for $(La_2Na)NaPtO_6$ was deposited previously under ICSD no. 281475.[8]

IC060105O

(35) Brown, I. D. http://www.ccp14.ac.uk/ccp/web-mirrors/i_d_brown and http://www.ccp14.ac.uk/ccp/web-mirrors/i_d_brown (April 2005).
(36) Shannon, R. D. *Acta Crystallogr.* **1976**, *A32*, 751.